



Winds on Titan from ground-based tracking of the Huygens probe

W. M. Folkner,¹ S. W. Asmar,¹ J. S. Border,¹ G. W. Franklin,¹ S. G. Finley,¹ J. Gorelik,¹ D. V. Johnston,¹ V. V. Kerzhanovich,¹ S. T. Lowe,¹ R. A. Preston,¹ M. K. Bird,² R. Dutta-Roy,² M. Allison,³ D. H. Atkinson,⁴ P. Edenhofer,⁵ D. Plettemeier,⁶ and G. L. Tyler⁷

Received 24 November 2005; revised 30 April 2006; accepted 4 May 2006; published 20 July 2006.

[1] Large radio telescopes on Earth tracked the radio signal transmitted by the Huygens probe during its mission at Titan. Frequency measurements were conducted as a part of the Huygens Doppler Wind Experiment (DWE) in order to derive the velocity of the probe in the direction to Earth. The DWE instrumentation on board Huygens consisted of an ultrastable oscillator which maintained the high Doppler stability required for a determination of probe horizontal motion during the atmospheric descent. A vertical profile of the zonal wind velocity in Titan's atmosphere was constructed from the Doppler data under the plausible assumption of generally small meridional wind, as validated by tracked images from the Huygens Descent Imager/Spectral Radiometer (DISR). We report here on improved results based on data with higher temporal resolution than that presented in the preliminary analysis by Bird et al. (2005), corroborating the first in situ measurement of Titan's atmospheric superrotation and a region of strong vertical shear reversal within the lower stratosphere. We also present the first high-resolution display and interpretation of the winds near the surface and planetary boundary layer.

Citation: Folkner, W. M., et al. (2006), Winds on Titan from ground-based tracking of the Huygens probe, *J. Geophys. Res.*, *111*, E07S02, doi:10.1029/2005JE002649.

1. Introduction

[2] The Doppler Wind Experiment (DWE) was one of the six scientific investigations conducted on the Huygens probe during its mission to Titan [Lebreton et al., 2005]. The DWE was intended to determine the height profile of the zonal wind velocity in Titan's atmosphere by measuring the Doppler shift associated with a radio signal transmitted from the probe and received on both the Cassini spacecraft and the Earth, thus determining the components of the probe's velocity in both directions [Bird et al., 2002]. The probe's transmitter and the receiver on Cassini were each equipped with an identical rubidium ultrastable oscillator (USO) in one of the two radio channels in order to achieve the required measurement accuracy for this investigation. Similar Doppler tracking measurements to estimate

Jupiter's vertical wind profile were successfully performed with the Galileo probe including probe signal reception on both the Galileo spacecraft [Atkinson et al., 1996; Atkinson, 2001] and the Earth [Folkner et al., 1997].

[3] The planned Doppler measurements on the Cassini orbiter were unsuccessful due to an error in configuring the receiver's ultrastable oscillator. (A second channel that did not utilize ultrastable oscillators successfully delivered telemetry data from the other instruments to the orbiter for relay to Earth.) Several large radio telescopes on Earth, however, were able to receive and record the Huygens radio signal. It was expected that the combined Cassini and ground-based tracking of Huygens would enable a separation of the zonal and meridional wind profiles, since a third component of the probe's velocity, the vertical descent rate, could be determined from in situ measurements on the probe. Although the projections of the probe's horizontal velocity in the directions to Cassini and to Earth were largely in the east-west direction, the angle between the two projections was approximately 20°, which was considered sufficient to allow an estimate of the meridional velocity under the original plan of the experiment.

[4] As a result of the loss of the DWE data on board Cassini, the ground-based Doppler measurements became the only available Huygens DWE data and formed the basis for the initial zonal wind profile reported by Bird et al. [2005]. With only one Doppler component available, this preliminary profile was derived under the assumption that the meridional wind speed was zero. A determination of the

¹Jet Propulsion Laboratory, California Institute of Technology, Pasadena, California, USA.

²Argelander-Institut für Astronomie, Universität Bonn, Bonn, Germany.

³NASA Goddard Institute for Space Studies, New York, USA.

⁴Department of Electrical and Computer Engineering, University of Idaho, Moscow, Idaho, USA.

⁵Institut für HF-Technik, Universität Bochum, Bochum, Germany.

⁶Elektrotechnisches Institut, Technische Universität Dresden, Dresden, Germany.

⁷Center for Radar Astronomy, Stanford University, Stanford, California, USA.

Huygens ground track on Titan from descent images shows that the meridional wind speed is less than a few m/s at altitudes below approximately 50 km [Tomasko *et al.*, 2005]. The probe altitude and descent velocity as a function of time were provided by a separate, project-managed, Descent Trajectory Working Group (DTWG), which used a combination of dynamical modeling and pressure/temperature measurements made during the descent [Lebreton *et al.*, 2005; Fulchignoni *et al.*, 2005].

[5] Here we report improved results from a new analysis based on Doppler estimates with higher temporal resolution than the data used by Bird *et al.* [2005]. The higher time (vertical) resolution improves our ability to (1) determine the existence and (if yes) the more exact extent of the near-surface planetary boundary layer, (2) determine the detailed vertical structure of the slow wind layer, where the gradient is quite strong, and (3) determine atmospheric motions on shorter time scales to learn more about probe dynamics (buffeting and coupled probe/parachute motions) and thus smaller-scale atmospheric turbulence. The present work also provides a more comprehensive description of the experiment, instrumentation, and data analysis, as well as the actual Doppler measurements.

2. Experiment Description

[6] The Huygens probe was released from the Cassini spacecraft on 25 December 2004 [Lebreton *et al.*, 2005]. It entered the atmosphere of Titan with a velocity of 6 km/s (relative to a nominally co-rotating atmosphere) on 14 January 2005 at 10:13:01 UTC (all times given in this paper are Earth receive times). A heat shield used to protect the probe during the initial deceleration was ejected after atmospheric entry and shortly after deployment of the main parachute. Radio transmission was started about 45 seconds after parachute deployment. Signals reached Earth 67 minutes later. After 15 minutes of descent under the main parachute, a second stabilizer parachute was deployed for the final descent. Huygens landed on Titan at 12:45:17 UTC, approximately 2.5 hours after entering the atmosphere. After landing the probe continued to transmit. The radio signal was recorded by Cassini until 13:57 UTC and by Earth radio telescopes up to 16:00 UTC.

[7] The Huygens descent was on the sun-lit, anti-Saturn hemisphere of Titan. Figure 1 shows the observation geometry as viewed from Earth at the start of radio transmission. Titan, with rotation period of 15.945 days, rotated by 2.32° about its spin axis during the descent. This rotation resulted in the landing site moving closer to the sub-Earth point shown in Figure 1 during the descent. The zonal winds carried the probe a net distance on Titan of 166 km, or 3.63° of longitude, eastward relative to Titan, over the course of the descent.

[8] The Huygens radio system utilized two channels to transmit data. Channel A transmission at 2.040 GHz was referenced to a rubidium ultrastable oscillator in order to provide a frequency reference sufficiently stable to achieve the required Doppler measurement accuracy. Channel B, at a frequency of 2.098 GHz and in opposite (circular) polarization to channel A, was driven by a temperature compensated crystal oscillator that was not stable enough for useful Doppler measurements. The relevant radio

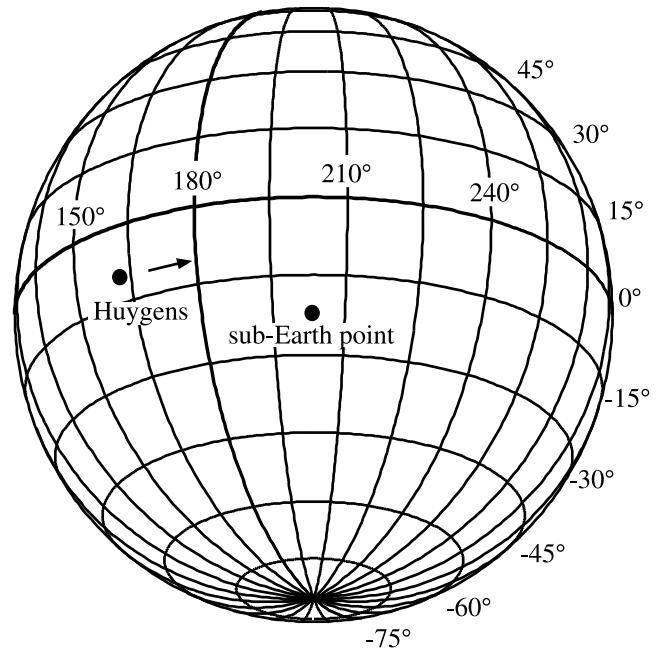


Figure 1. Ground-based DWE geometry. The Titan disk is shown as viewed from Earth at the start of radio transmission from the probe at latitude 10.3°S , longitude 164.1°E . The sub-Titan coordinates of Earth were latitude 22.6°S , longitude 203.1°E . As viewed from Huygens, the Earth was at elevation 56.1° , azimuth 115.3° . The measured Doppler shift of the radio signal is proportional to the projection of the velocity of the probe onto the direction to Earth. An eastward (relative to the surface) velocity of the probe of magnitude 1 m/s has a projection in the direction to Earth of -0.505 m/s. Similarly, a northward motion or an upward velocity of 1 m/s have projections in the direction to Earth of 0.239 m/s and -0.830 m/s, respectively.

parameters of the experiment are summarized in Table 1. The antenna was fixed to the body of the spinning probe and pointed vertically upward along the nominal spin axis. The antenna gain pattern, a measure affecting the strength of the signal in a given direction, was fairly broad with a peak of 5 dB and a gain of about 4 dB in the direction of the Earth.

[9] Reliable detection of the Huygens signal at Earth required the use of antennas of diameter 50 m or greater with receivers operating at the Huygens transmission frequency. With no single such radio telescope on Earth able to view Titan for the entire probe descent, a combination of several telescopes was used. The 100 m diameter Robert C. Byrd Green Bank Telescope (GBT) in West Virginia was used to observe the initial part of the descent. The 64 m diameter Parkes Telescope in Australia was used to observe the final part of the descent and an extended period of time after the probe had landed. An interval of approximately 24 minutes of the descent was not observable by either large telescope. Four 25 m diameter telescopes of the Very Long Baseline Array (VLBA) in the USA were enlisted to fill in this period: Pie Town, Owens Valley, Mauna Kea, and Kitt Peak. In principle, the signals from the four small antennas can be combined to an equivalent 50 m diameter antenna. In that case, the combined signal-to-noise ratio would still be significantly

Table 1. Huygens-to-Earth Radio Link Parameters

Parameter	Value
Huygens Transmission	
RF power, each channel, W	11.6
Chain A frequency, MHz	2040.0
Chain A polarization	LCP
Chain A frequency reference	Rb USO
Chain B frequency, MHz	2097.9
Chain B polarization	RCP
Chain B frequency reference	crystal oscillator
Data rate, each channel, bits/s	8192
Carrier suppression, dB	-4.45
Ultrastable Oscillator (USO)	
Output frequency, MHz	10
Warm-up time, hours	0.5
Drift stability $\delta f/f$ (30 min)	2×10^{-10}
Probe Antenna	
Type	helix
Average gain in direction to Earth, dBi	4
3 dB beam width, degree	120
Transmission losses, dB	0.4
Distance to Earth, AU	8.05
Green Bank Telescope	
Diameter, m	100
Efficiency	0.7
Noise temperature, K	30
Received carrier power, W	2.8×10^{-21}
Parkes Telescope	
Diameter, m	64
Efficiency	0.5
Noise temperature, K	30
Received carrier power, W	7.2×10^{-22}

smaller than that obtained at Green Bank or at Parkes, and would be just barely detectable. If the telemetry modulating the signal had been recovered, the received signal could have been demodulated and resulted in an easily detectable signal. In the absence of the telemetry, our efforts to combine the signals have shown that the signal was detected but has not yet been modeled well enough to extract useful Doppler measurements. We hope that further modeling will eventually be successful.

[10] These six telescopes were also a subset of a larger network participating in Very Long Baseline Interferometry (VLBI) observations for the purpose of determining the probe's precise position on the sky [Pogrebenko *et al.*, 2004; Lebreton *et al.*, 2005]. The overview paper by Witasse *et al.* [2006] summarizes the VLBI experiment and facilities used. The sharing of resources for the Doppler experiment with the VLBI experiment resulted in compromises on the resulting measurements. The VLBI experiment calibration required that the telescopes alternately point at Titan and at an extragalactic radio source over a three-minute cycle, of which about 100 seconds were available for Huygens tracking.

3. Signal Processing

[11] At each telescope, the Huygens signal at frequency 2.040 GHz was multiplied by a fixed local oscillator of frequency 2.0403 GHz to down-convert the signal to a frequency of approximately 300 kHz. This was sampled at a rate of 1.25 MHz with 8 bit resolution.

[12] The recorded samples were processed to determine the frequency of the received signal. A model for the expected signal phase as a function of time t ,

$$\phi_m(t) = 2\pi(x/\lambda - f_0 t) \quad (1)$$

was constructed using the nominal value of the transmission frequency f_0 and wavelength λ and the distance x between the probe and the radio telescopes from nominal values of the orbits and rotation of Titan and Earth. The signal sampled voltage $V(t_n)$ at time t_n was multiplied by cosine and sine of the model phase ϕ_m to generate a time series of signal components in-phase and out-of phase with the phase model, I_n and Q_n .

$$I_n = V(t_n) \cos(\phi_m(t_n)) \quad (2)$$

$$Q_n = -V(t_n) \sin(\phi_m(t_n)) \quad (3)$$

[13] The time series of I_n and Q_n would be constant except for small errors in the phase model due to wind or any other effect not included in the phase model. The residual frequency was estimated by forming the power spectrum of the complex time series of $I_n + iQ_n$ over a given integration time. In general the time interval is chosen to be long enough to obtain acceptable signal-to-noise and frequency resolution while being short enough to provide adequate temporal resolution. The integration time cannot be longer than the time over which the model fits the real signal to a fraction of a radian of phase. For weak signals and/or large unknowns in the phase model, better detection can be achieved by averaging several consecutive power spectra.

[14] The final results were obtained using integration times of 2 s at GBT, 3 s at Parkes for the time before landing and 5 s at Parkes after landing, with no averaging of spectra. For each time interval, the phase model was formed from a dynamical model of the predicted motion of the probe combined with a linear change of frequency over the time interval. The frequency rate was varied independently for each time interval as necessary to give the highest signal-to-noise ratio (SNR). The typical SNR for each interval was about 4 for the chosen integration times. Samples of the resulting estimates are shown in Figure 2. The best fit for the frequency rate sometimes agrees well with the trend in the frequency estimates (Figure 2a). For other intervals the best fit frequency rate does not match up with the change in estimated frequency over time (Figure 2b). This could be due to effects that changed the phase of the radio signal over time scales shorter than 2 s, such as variation in the probe spin rate, coupled oscillations of the probe/parachute system, buffeting from wind gusts, etc., and/or to fluctuations in the delay due to atmospheric effects.

[15] Figure 3 shows the estimated frequency as a function of time as measured at GBT and Parkes. The largest change in Doppler shift over the descent period is due to the change in relative velocity of Earth and Titan; the changing Doppler due to rotation of the Earth (approximately 3 kHz) is evident in the change in frequency between the last measurement made at GBT (at which Titan was setting below the horizon) and the first point measured at Parkes (at which Titan was

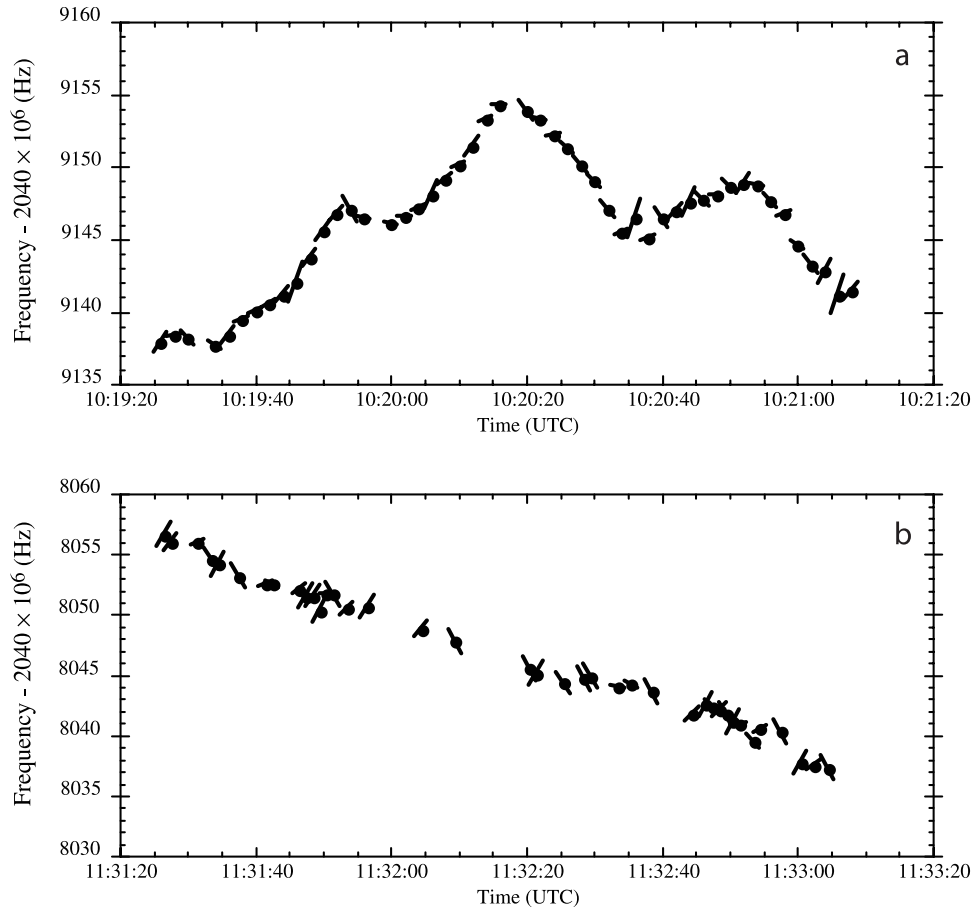


Figure 2. High-resolution Doppler measurements for two 100 s intervals at the Green Bank Telescope. The frequency and the linear frequency rate (bar through each point) yielding the highest signal-to-noise ratio were determined for successive 2 s time intervals. (a) Example during descent under the main parachute (altitude ~ 140 km), where the estimated frequency rate agrees with the trend apparent in adjacent time intervals. (b) Example during descent under the stabilizer parachute (altitude ~ 26 km), where the agreement between frequency rate and adjacent-interval change in frequency is poor. The disagreement is probably due to rapid probe dynamics, i.e., turbulence buffeting and/or parachute swing.

rising). Distinct probe dynamics are clearly visible during the early part of the descent. The landing is just apparent shortly after the start of measurements at Parkes. There is a gap of approximately 24 minutes in the data between the end of the track at GBT and the start of the track at Parkes when Titan was not in view of either telescope. Another gap in the data occurred a few hours after the probe landing where the antenna was pointed at an extragalactic radio source for calibration of the VLBI experiment. The measurements ended when Titan could no longer be tracked at Parkes.

[16] Figure 4 shows the Doppler measurement residuals (measured minus model frequency) to a fit of the post-landed data. The landed Doppler data combined with the integrated descent trajectory determine the landing position to be latitude 10.33°S , longitude 192.32°W (167.68°E). The standard deviation of the Doppler residuals in Figure 4 is 0.11 Hz. This measurement noise is consistent with in-flight test data and is limited by the stability of the locking of the radio transmitter signal to the ultrastable oscillator. The measurement noise represents the best possible accuracy with which the wind profile could be estimated, corresponding to ± 16 mm/s in radial velocity. Systematic effects result in larger

uncertainty in the zonal wind speed, which we estimate to have accuracy of 80 cm/s near the start of descent and 15 cm/s shortly before landing. Details of the systematic uncertainties are given by *Dutta-Roy and Bird* [2004].

4. Profile of Winds on Titan

[17] The zonal wind speed as a function of altitude down to the surface of Titan, as derived from the ground-based Doppler measurements, is shown in Figure 5. As described above, the sampling time for this profile has been decreased (to 2–3 s) compared with that of the preliminary profile (10 s) by *Bird et al.* [2005]. Also shown in Figure 5 are wind profiles computed from General Circulation Model (GCM) simulations of Titan. The GCM results, from *Hourdin et al.* [1995] and *Luz et al.* [2003], are for the latitude of the Huygens descent and for the northern winter solstice season (Sun orbital longitude $L_s = 270^\circ$). The Huygens descent was somewhat later in the seasonal cycle ($L_s \sim 300^\circ$).

[18] The zonal wind profile in Figure 5 was estimated with the assumption of no meridional wind speed. The descent images show that the meridional wind speed is low for altitudes below approximately 50 km. Figure 6, adapted

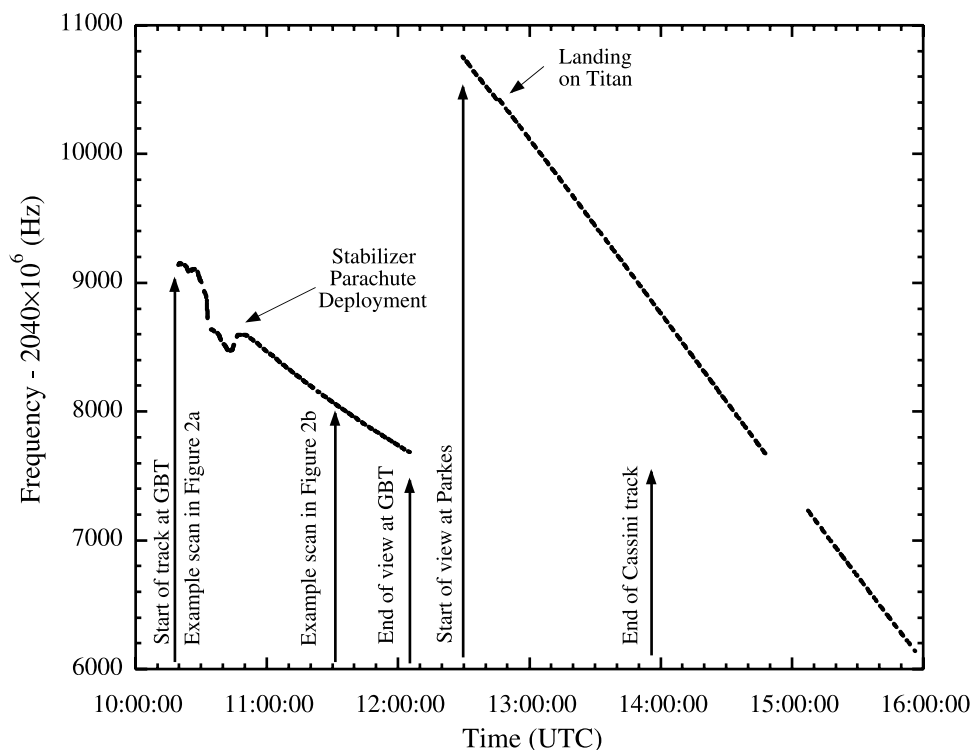


Figure 3. Measured sky frequency of the Huygens probe radio signal at both GBT and Parkes. A constant offset of 2.04 GHz (transmitted frequency) has been subtracted. The Earth's rotation is primarily responsible for the lower recorded frequency at GBT (near end of track) with respect to Parkes (near start of track). A gap during the descent of some 24 minutes exists between the GBT and Parkes data recording intervals. The small gaps between data segments and the larger post-landing gap correspond to intervals when the radio telescopes were pointed to celestial reference sources near Titan for calibration of the simultaneously conducted VLBI experiment. The times of impact at 12:45:17 UTC and loss of link to Cassini at 13:57:31 UTC are indicated. The Parkes tracking pass ended at 16:00 UTC with the Huygens probe still transmitting from the Titan surface.

from Tomasko *et al.* [2005], shows the wind direction derived from the descent images. Between altitudes of 10 km and 50 km the wind direction is seen to be within 10° of east. For altitudes below 10 km the wind speed reverses from eastward to westward. In this range the total wind velocity is small, less than 5 m/s, and the angle deviation from westward is about 30° , indicating a meridional wind speed of about half that of the zonal wind speed. At altitudes above 50 km, the meridional wind profile may yet be estimated by the VLBI experiment. Other possible errors in the zonal wind velocity estimates are related to the uncertainties in the descent rate and in the landed position, which are expected to be reduced with further processing of the various data sets.

[19] The estimated wind profile shows a sharp drop in wind speed to near zero at an altitude between 60 km and 75 km, or approximately 40 hPa and 20 hPa, defining a region of strong reversed shear at 40 hPa under a region of strong prograde shear between 75 km and 100 km. The wind shear shows a decrease in the zonal wind speed by 40 m/s and then back up again by 40 m/s over a time interval of 15 minutes. This feature appears at an altitude where slight wind shear was computed in the models of Luz *et al.* [2003] and Hourdin *et al.* [1995]. The observed shear is much stronger than in the simulations. Our profile assumes that the wind speed is purely zonal, which is known

from the descent imaging to be a very good approximation up to 50 km altitude (see Figure 6). If instead the wind shear was meridional and the zonal wind was roughly constant over that 15 minute time interval, the Doppler measurements could have been produced by a northward meridional wind that grew swiftly to 90 m/s and then receded back to zero within 15 minutes. It seems more likely that the wind shear is zonal. The results from the VLBI experiment may be able to confirm this. In any case a strong wind shear is certain.

[20] The cause of this reversed shear region bears further study, but is probably related to the vertical maximum in the static stability at the same altitude within Titan's lower stratosphere, according to the measured vertical profiles of temperature [Lindal *et al.*, 1983; Fulchignoni *et al.*, 2005], which modulates the efficiency of the advective and eddy transports of both thermal energy and momentum. As shown in the models of Luz *et al.* [2003] and Hourdin *et al.* [1995], the inflected vertical shear region in the GCM simulations is bounded from above by a vertically segregated region of the pole-to-pole Hadley circulation. The rising motion near the south pole, sinking near the north, flows northward at 30–50 hPa, but is surmounted by southward flow across the equator just above, itself the lower portion of a vertically distinct pole-to-pole cell extending to the top of the model domains. This stacked cell structure, as enforced by the radiatively imposed

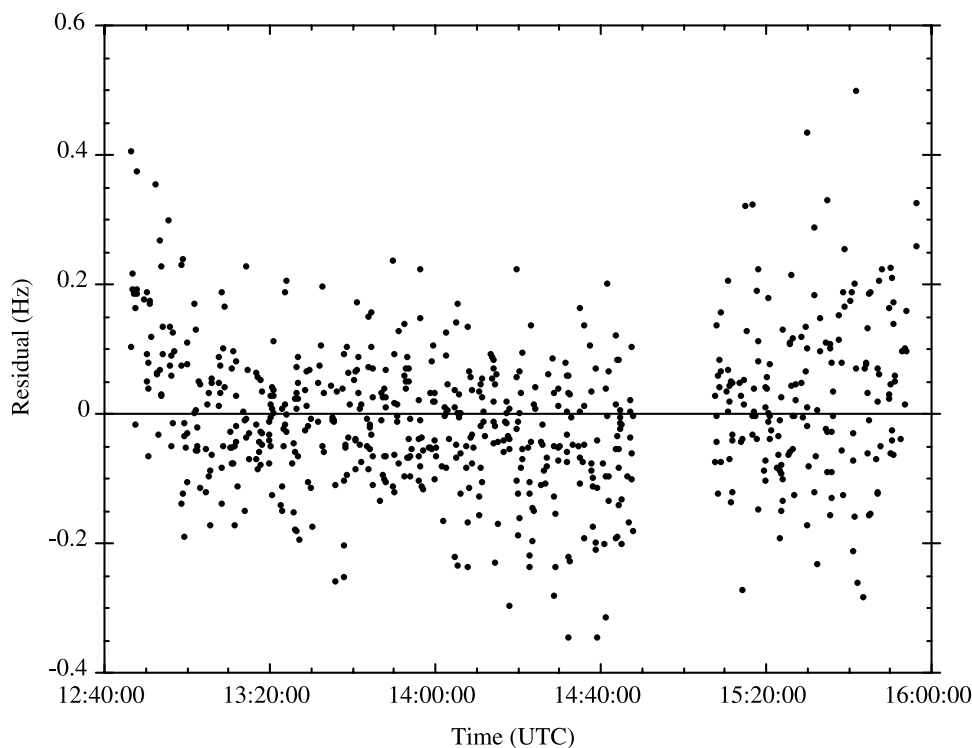


Figure 4. Doppler frequency residuals for post-landing measurements after subtracting a long-term drift. The standard deviation of the landed frequency measurements is 0.11 Hz, corresponding to ± 16 mm/s in radial velocity.

vertical maximum in the static stability, may in turn impose the vertical alternation of wind shear in this region. The reversed shear zone may also be due to the effect of momentum damping by vertically propagating waves or to gravitational tides [Walterscheid and Schubert, 2006].

[21] Further analysis of the residual small-scale variation of the measured Doppler frequency and correlated temperature variations measured by the Huygens Atmospheric Structure Instrument [Fulchignoni *et al.*, 2005] could provide a diagnostic constraint on this process. If, for example, a regular vertical wavelength and amplitude can be detected along with their variation with altitude, as in the related work on the Galileo Doppler experiment at Jupiter [Allison and Atkinson, 2001], then such structure may be associated with a particular gravitational wave mode. Once identified, the dispersive properties of any such mode as constrained by linear wave theory for the indicated background flow and vertical shear, may suggest an estimate of the wave-induced deceleration of the flow [cf. Lindzen, 1981]. Alternatively, this issue might be addressed with the incorporation of a tunable wave-drag parameterization or the explicit resolution of momentum fluxes by small-scale waves in an advanced Titan GCM, as yet lacking in the published models. By this approach numerical modelers might attempt to vary the adjustable parameters or assumed forcing representation of these processes until the vertical structure of the simulated zonal flow bears a closer resemblance to our measured profile.

[22] Figure 7 shows the profile of the lowest 5 km altitude. The wind speed is slow and retrograde between 1 km and 5 km altitude, reversing to slightly prograde at

the surface. As already noted by Bird *et al.* [2005], the low-altitude vertical shear of the DWE profile, with wind speed increasingly westward with increasing altitude, could indicate the thermal wind balance of warmer-poleward temperatures in the lower atmosphere during southern summer solstice, consistent with the generation of episodic cloud-convective centers near the south pole [Brown *et al.*, 2002]. If such a warmer-poleward region is supported by the seasonal surface heating, the roughly 3 km height of this reversed shear zone may be indicative of the height of a convectively well-mixed layer. This would appear to be consistent with the indication of an approximately uniform mixing ratio of CH_4 measured by the Huygens Gas Chromatograph Mass Spectrometer below 5 km altitude [Niemann *et al.*, 2005]. It is interesting that the Titan GCM simulation of Tokano and Neubauer [2005] for the Huygens landing date shows a very thin region of eastward surface flow surmounted above by weak westward winds of approximately 2 m/s. This would be consistent with the results retrieved from the Parkes data.

[23] The ≈ 1 m/s eastward surface wind is consistent with the theoretical prediction [Flasar and Conrath, 1992; Allison, 1992] of a surface gradient-wind less than 2 m/s. The inferred eastward direction of the surface flow would be consistent with the indicated direction of possible surface wind gusts associated with the morphology of low-latitude surface streaks observed by Cassini imaging [Porco *et al.*, 2004]. Eastward surface flow at southern low-latitudes would also be dynamically consistent with the Coriolis deflection there of a southward, cross-equatorial Hadley circulation, as simulated

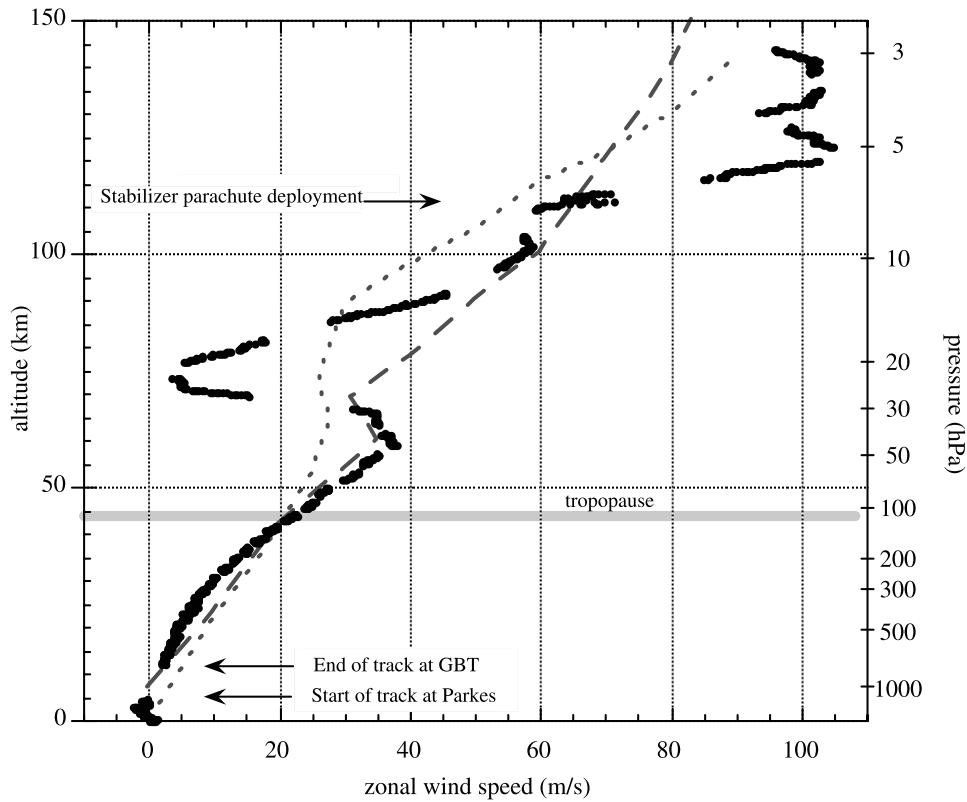


Figure 5. Vertical profile of Titan zonal wind from improved DWE frequency estimates at mean integration times of 2–3 s, shown as points for the individual measurements. Also shown are results from general circulation models. The dashed line is adapted from Figure 6 of *Hourdin et al.* [1995]. The dotted line is adapted from Figure 8 of *Luz et al.* [2003]. On the scale of the entire descent, the higher time resolution produces only minor changes with respect to the preliminary profile derived by *Bird et al.* [2005]. The uncertainties remain near 80 cm/s near the start of descent and 15 cm/s shortly before landing. The wind shear layer between 60 km and 100 km is coincident with the steep vertical temperature gradient measured in situ on Huygens [*Fulchignoni et al.*, 2005].

for the southern summer season by Titan GCMs [*Luz et al.*, 2003; *Hourdin et al.*, 1995].

[24] The Huygens landing location, near the equator, and Titan orbit phase, 12.9 Earth days after periapsis, was in a region where gravitational tidal winds were expected to be low. In a model by *Tokano and Neubauer* [2002], Huygens might have been expected to experience a small northwestward-directed tidal wind. The observed near surface winds were comparable in magnitude. However, it would be premature to draw conclusions on the drivers of the large-scale circulation on Titan from the height profile of a single descent probe, especially in a region where tidal effects were expected to be small. Experimental verification of the effects due to tidal winds remains a goal for future exploration, most efficiently with a fleet of passive balloons released at various different Titan latitudes [*Tokano and Lorenz*, 2006].

5. Conclusion

[25] Improved results have been obtained of the vertical profile of the zonal wind on Titan based on data with higher temporal resolution than those reported earlier. The wind profile shows an unanticipated drop in wind speed in a region of strong reversed shear toward weaker-upward flow

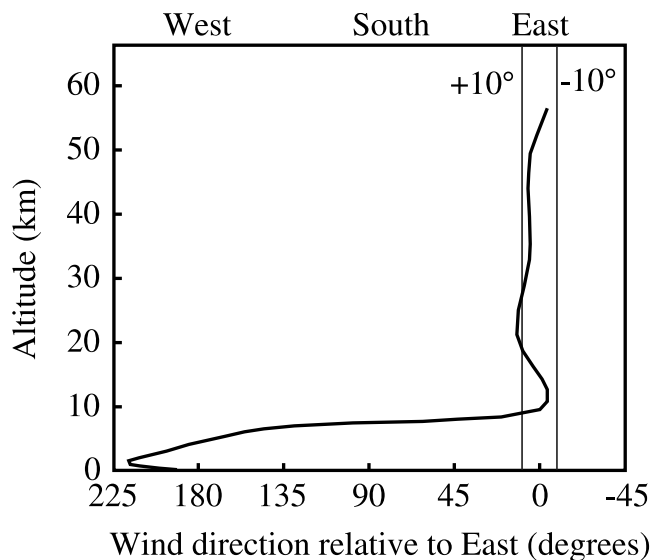


Figure 6. Horizontal wind speed direction derived from Huygens descent images (adapted by permission from Macmillan Publishers Ltd from *Tomasko et al.* [2005]).

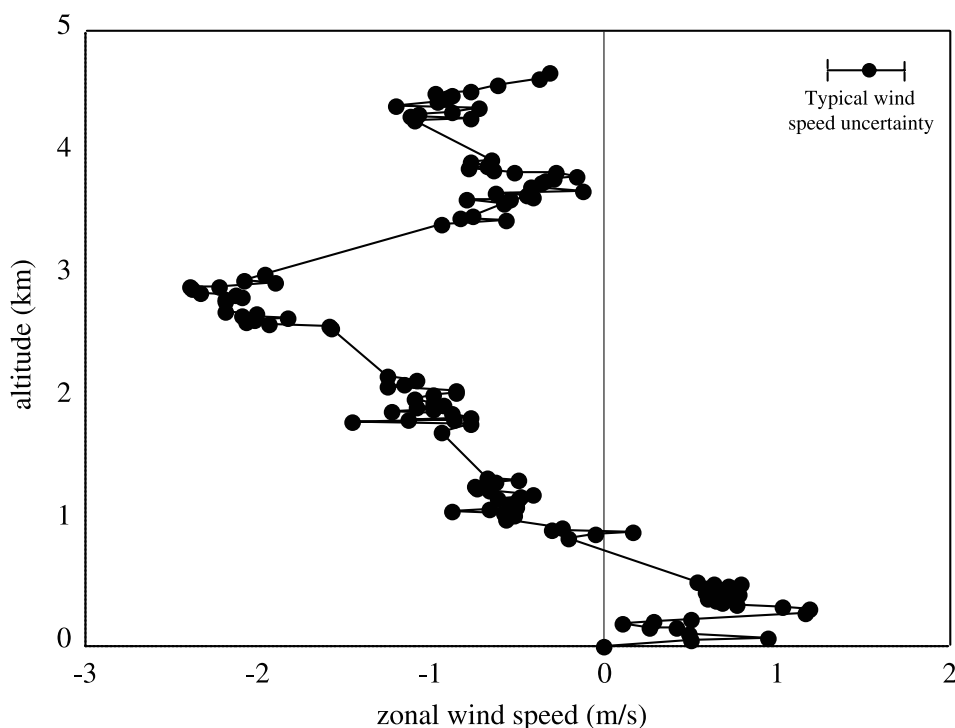


Figure 7. Vertical zonal wind profile during the last 5 km of descent. The wind at the surface of Titan is an eastward breeze (prograde) that switches direction and becomes a weak westward wind (retrograde) at about 1 km altitude. This trend, which continues up to the start of the Parkes measurements at about 4.8 km, has been verified by ground track determinations from Huygens images [Tomasko et al., 2005].

with strong prograde shear aloft. This may be related to the vertical maximum in the static stability at the same altitude within Titan's lower stratosphere, or to the possibility that the reversed shear zone is the effect of momentum damping by vertically propagating waves. The wind speed is slow and retrograde between 1 km and 5 km altitude, reversing to slightly prograde at the surface, possibly indicating the thermal wind balance of warmer-poleward temperatures in the lower atmosphere during southern summer solstice. Future work will include filling the gap in the ground-based observations between the Green Bank and Parkes view periods as well as inclusion of VLBI results and constraints on meridional motion in the upper atmosphere. Further analysis of the residual small-scale variation of the measured Doppler frequency may provide a diagnostic constraint on the process generating the wind shear layer.

[26] **Acknowledgments.** The authors thank the following colleagues for their assistance in carrying out this experiment: Jim Ulvestad, Jon Romney, Don Haenichen, Paul Rhodes, Mark McKinnon, Ray McFarlin, Duane Clark, Jim Brown, Frank Ghigo, Bill Robins, Bill Hancock, and Tony Sylvester from the National Radio Astronomy Observatory for their assistance in the use of the Robert C. Byrd Green Bank Telescope and antennas of the Very Long Baseline Array, John Reynolds, John Sarkissian, and Tasso Tzioumis for their assistance in the use of the Parkes telescope operated by the Australia Telescope National Facility, Leonid Gurvits, Sergei Pogrebenko and Ian Avruch for their collaborative use of the radio antennas and for the creation of schedule files, Lindley Johnson and Bery Geldzahler of NASA, and Charles Elachi, Robert Mitchell, and William Weber of the Jet Propulsion Laboratory for their encouragement and financial support. We also thank Aseel Anabtawi and Andre Jongeling of the Jet Propulsion Laboratory for technical and operations support. The extensive and constructive comments by the anonymous reviewer are gratefully acknowledged. This research was carried out in part at the Jet Propulsion

Laboratory, California Institute of Technology, under contract with the National Aeronautics and Space Administration, and presents results of a research project partially funded by the Deutsches Zentrum für Luft- und Raumfahrt.

References

- Allison, M. (1992), A preliminary assessment of the Titan planetary boundary layer, in *Proceedings of the Symposium on Titan, Eur. Space Agency Spec. Publ., ESA SP-338*, 113–118.
- Allison, M., and D. H. Atkinson (2001), Galileo Probe Doppler residuals as the wave-dynamical signature of weakly stable, downward increasing stratification in Jupiter's deep wind layer, *Geophys. Res. Lett.*, *28*, 2747–2750.
- Atkinson, D. H. (2001), The Galileo Jupiter Probe Doppler Wind Experiment, *Sol. Syst. Res.*, *35*, 387–413.
- Atkinson, D. H., J. B. Pollack, and A. Seiff (1996), Galileo Doppler measurements of the deep zonal winds at Jupiter, *Science*, *272*, 842–843.
- Bird, M. K., et al. (2002), The Huygens Doppler Wind Experiment — Titan winds derived from probe radio frequency measurements, *Space Sci. Rev.*, *104*, 613–640.
- Bird, M. K., et al. (2005), The vertical profile of winds on Titan, *Nature*, *438*, 800–802.
- Brown, M. E., A. H. Bouchez, and C. A. Griffith (2002), Direct detection of variable tropospheric clouds near Titan's south pole, *Nature*, *420*, 795–797.
- Dutta-Roy, R., and M. Bird (2004), A Titan zonal wind retrieval algorithm, in *Proceedings of the International Workshop on Planetary Probe Atmospheric Entry and Descent Trajectory Analysis and Science*, edited by A. Wilson, *Eur. Space Agency Spec. Publ., ESA SP-544*, 109–116.
- Flasar, F. M., and B. J. Conrath (1992), The meteorology of Titan, in *Proceedings of the Symposium on Titan, Eur. Space Agency Spec. Publ., ESA SP-338*, 89–99.
- Folkner, W. M., R. A. Preston, J. S. Border, J. Navarro, W. Wilson, and M. Oestreich (1997), Earth-based radio tracking of the Galileo Probe for Jupiter wind estimation, *Science*, *275*, 644–646.
- Fulchignoni, M., et al. (2005), In situ measurements of the physical characteristics of Titan's environment, *Nature*, *438*, 785–791.

- Hourdin, F., O. Talagrand, R. Sadourny, R. Courtin, D. Gautier, and C. P. McKay (1995), Numerical simulation of the general circulation of the atmosphere of Titan, *Icarus*, *117*, 358–374.
- Lebreton, J. P., et al. (2005), An overview of the descent and landing of the Huygens probe on Titan, *Nature*, *438*, 758–764.
- Lindal, G. F., G. E. Wood, H. B. Holtz, D. N. Sweetnam, V. R. Eshleman, and G. L. Tyler (1983), The atmosphere of Titan: An analysis of the Voyager 1 radio occultation measurements, *Icarus*, *53*, 348–363.
- Lindzen, R. S. (1981), Turbulence and stress owing to gravity-wave and tidal breakdown, *J. Geophys. Res.*, *86*, 9707–9714.
- Luz, D., F. Hourdin, P. Rannou, and S. Lebonnois (2003), Latitudinal transport by barotropic waves in Titan's stratosphere. II. Results from a coupled dynamics-microphysics-photochemistry GCM, *Icarus*, *166*, 343–358.
- Niemann, H. B., et al. (2005), The abundances and constituents of Titan's atmosphere from the GCMS instrument on the Huygens probe, *Nature*, *438*, 779–784.
- Pogrebenko, S. V., L. I. Gurvits, R. M. Campbell, I. M. Avruch, J.-P. Lebreton, and C. G. M. van't Klooster (2004), VLBI tracking of the Huygens probe in the atmosphere of Titan, in *Proceedings of the International Workshop on Planetary Probe Atmospheric Entry and Descent Trajectory Analysis and Science*, edited by A. Wilson, *Eur. Space Agency Spec. Publ., ESA SP-544*, 197–204.
- Porco, C. C., et al. (2004), Imaging of Titan from the Cassini spacecraft, *Nature*, *434*, 159–168.
- Tokano, T., and R. D. Lorenz (2006), GCM simulation of balloon trajectories on Titan, *Planet. Space Sci.*, in press.
- Tokano, T., and F. M. Neubauer (2002), Tidal winds on Titan caused by Saturn, *Icarus*, *158*, 499–515.
- Tokano, T., and F. M. Neubauer (2005), Wind-induced seasonal angular momentum exchange at Titan's surface and its influence on Titan's length-of-day, *Geophys. Res. Lett.*, *32*, L24203, doi:10.1029/2005GL024456.
- Tomasko, M. G., et al. (2005), Rain, winds and haze during the Huygens probe's descent to Titan's surface, *Nature*, *438*, 765–778.
- Walterscheid, R. L., and G. Schubert (2006), A tidal explanation for the Titan haze layers, *Icarus*, doi:10.1016/j.icarus.2006.03.001, in press.
- Witasse, O., et al. (2006), Overview of the coordinated ground-based observations of Titan during the Huygens mission, *J. Geophys. Res.*, doi:10.1029/2005JE002640, in press.
-
- M. Allison, NASA Goddard Institute for Space Studies, 2880 Broadway, New York, NY 10025, USA.
- S. W. Asmar, J. S. Border, S. G. Finley, W. M. Folkner, G. W. Franklin, J. Gorelik, D. V. Johnston, V. V. Kerzhanovich, S. T. Lowe, and R. A. Preston, Jet Propulsion Laboratory, 4800 Oak Grove Drive, Mail Stop 301-460, Pasadena, CA 91001, USA. (william.folkner@jpl.nasa.gov)
- D. H. Atkinson, Department of Electrical and Computer Engineering, University of Idaho, Moscow, ID 83844-1023, USA.
- M. K. Bird and R. Dutta-Roy, Argelander-Institut für Astronomie, Universität Bonn, Auf dem Hügel 71, D-53125 Bonn, Germany.
- P. Edenhofer, Institut für HF-Technik, Universität Bochum, D-44780 Bochum, Germany.
- D. Plettemeier, Elektrotechnisches Institut, Technische Universität Dresden, D-01062 Dresden, Germany.
- G. L. Tyler, Center for Radar Astronomy, Stanford University, Stanford, CA 94305, USA.